Precise computation of the direct and indirect topographic effects of Helmert's 2nd method of condensation using SRTM30 digital elevation model

Research article

Y. M. Wang¹*

1 National Geodetic Survey 1315 East West HYW, Silver Spring, MD 20910 USA

Abstract

The direct topographic effect (DTE) and indirect topographic effect (ITE) of Helmert's 2nd method of condensation are computed using the digital elevation model (DEM) SRTM30 in 30 arc-seconds globally. The computations assume a constant density of the topographic masses. Closed formulas are used in the inner zone of half degree, and Nagy's formulas are used in the innermost column to treat the singularity of integrals. To speed up the computations, 1-dimensional fast Fourier transform (1D FFT) is applied in outer zone computations. The computation accuracy is limited to 0.1 mGal and 0.1cm for the direct and indirect effect, respectively.

The mean value and standard deviation of the DTE are -0.8 and \pm 7.6 mGal over land areas. The extreme value -274.3 mGal is located at latitude -13.579° and longitude 289.496°, at the height of 1426 meter in the Andes Mountains. The ITE is negative everywhere and has its minimum of -235.9 cm at the peak of Himalayas (8685 meter). The standard deviation and mean value over land areas are \pm 15.6 cm and -6.4 cm, respectively. Because the Stokes kernel does not contain the zero and first degree spherical harmonics, the mean value of the ITE can't be compensated through the remove-restore procedure under the Stokes-Helmert scheme, and careful treatment of the mean value in the ITE is required.

Keywords:

Helmert's 2nd method of condensation • topographic effect • indirect effect • direct effect • SRTM digital elevation model © Versita sp. z o.o.

Received 25-04-2011; accepted 01-07-2011

1. Introduction

Under the assumption of non-variation of the topographic mass along the radius direction, the topographic potential and its derivatives can be reduced from 3-dimensional Newtonian integrals into 2-dimnensional surface integrals with closed kernel functions (Martinec, 1998; Sjöberg and Nahavandchi, 1999; Smith et al., 2001; Heck, 2003). Based on these integrals, the DTE and ITE are computed by using SRTM30 global elevation model (Becker et al., 2009) in 30" resolution.

The computations of DTE and ITE are global integrations. It becomes impractical when a very high resolution DEM, such as the STRM30, is used. Usually, the closed kernel functions are expanded into Taylor series, so that the most efficient 1D FFT can be applied. However, Taylor series do not converge near the computation point in mountainous areas, for the topographic height becomes larger than distance between the computation and current points. To overcome this difficulty, we split the computations into an inner zone of half by half degree block and an outer zone for the rest of the globe. In the inner zone, the closed formulas are used; for the outer zone computations, the closed formulas are expanded into Taylor series and 1D FFT is utilized. The computation errors are limited to below 0.1 cm and 0.1 mGal for the ITE and direct effect,



^{*}E-mail: Yan.wang@noaa.gov

respectively.

2. Computation formulas for DTE and ITE of Helmert's $\mathbf{2}^{nd}$ method of condensation

If we assume the density of the Earth's topographic mass is a function of latitude and longitude only, the gravitational potential of the topography at any given point *P* can be computed by a surface integral (e.g., Martinec, 1998; Sjöberg and Nahavandchi, 1999; Smith et al., 2001; Heck, 2003):

$$V_P(\phi, \lambda) = G \iint_{\sigma} \rho(\phi, \lambda) k(r_S, r_G, r_P, \psi) d\sigma \tag{1}$$

where G is Newton's gravitational constant, r_P is the radial distance of the computation point P, r_S is the radial distance to a point on the Earth surface, r_G is the radial distance to a point on the geoid, ρ is the density of the mass element, σ is the unit sphere, and k is the kernel function given by:

$$k = \left(\frac{3rp\cos\psi}{2} + \frac{r_S}{2}\right)l_{SP} - \left(\frac{3rp\cos\psi}{2} + \frac{r_G}{2}\right)l_{GP}$$

$$+ \frac{1}{2}(-1 + 3\cos^2\psi)r_P^2 \ln\frac{r_S - r_P\cos\psi + l_{SP}}{r_C - r_P\cos\psi + l_{CP}}$$
(2)

where l_{SP} and l_{GP} are distances between points, and the subscripts S and G denote the points on the Earth's surface and the geoid, respectively. The distances are given by:

$$l_{SP} = \sqrt{r_S^2 - 2r_S r_P \cos \psi + r_P^2}$$
 (3)

$$l_{GP} = \sqrt{r_G^2 - 2r_G r_P \cos \psi + r_P^2}$$
 (4)

We dropped the absolute sign in the natural logarithm in the kernel function (2). The sign is unnecessary (see appendix).

The vertical attraction of topography g_t can be computed by a surface integral as (ibid.)

$$g_{t}(\phi,\lambda) = G \iint_{\sigma} \rho(\phi,\lambda) k'(r_{S}, r_{G}, r_{P}, \psi) d\sigma \qquad (5)$$

where the kernel function k' is given by

$$k'(r_{P}, r_{G}, r_{S}, \psi) = -\frac{\partial k}{\partial r_{P}}$$

$$= -\frac{r_{S}r_{P}(1 - 6\cos^{2}\psi) + (3r_{P}^{2} + r_{S}^{2})\cos\psi}{l_{SP}}$$

$$+ \frac{r_{G}r_{P}(1 - 6\cos^{2}\psi) + (3r_{P}^{2} + r_{G}^{2})\cos\psi}{l_{GP}}$$
(6)

$$-(-1+3\cos^2\psi)r_P\ln\frac{r_S-r_P\cos\psi+l_{SP}}{r_G-r_P\cos\psi+l_{GP}}$$

VERSITA

The potential and gravity of the topography can be evaluated rigorously at any given point using Eqs. (2) - (6), provided that the density of the topographic mass, the surfaces of the Earth and the geoid are known.

Since the maximum value of ITE is about 2.5 meters, the ellipsoidal effect is in mm level and is ignored in this paper. The spherical approximation is used hereafter in the following formulations.

After the topographic masses are condensed onto the geoid (Helmert's 2^{nd} method of condensation), the gravitational potential of the condensed surface layer at the point P is (Moritz, 1968, Eq. 56):

$$V_S(\phi, \lambda) = GR^2 \iint_{\sigma} \rho(\phi', \lambda') \frac{H}{l_{GP}} d\sigma$$
 (7)

where H is the orthometric height.

For mass conservation, a local density function is introduced (e.g., Heck, 2003):

$$\rho' = \rho(\phi, \lambda)[1 + \frac{H}{R} + \frac{1}{3}(\frac{H}{R})^2]$$
 (8)

The attraction of the condensed layer g_S at point P is given by differentiating Eq. (7) respect to r_P :

$$g_S(\phi, \lambda) = -\frac{\partial V_S}{\partial r_P} = GR^2 \iint_{\sigma} \rho(\phi', \lambda') H \frac{r_P - r_G \cos \psi}{l_{GP}^3} d\sigma$$
(9)

The ITE is defined as the geoid change due to the shifting of masses to the condensation layer. For the ITE computation, the point P is on the geoid and $r_P = R$. The ITE can be compute in the same form as Eq. (1) by using the kernel function (cf. Martinec, 1998; Sjöberg and Nahavandchi, 1999)

$$k_{ITE} = \gamma^{-1} \left\{ \frac{3R\cos\psi + r_S}{2} l_{SR} - \frac{1+3\cos\psi}{2} R l + \frac{1}{2} (-1 + 3\cos^2\psi) R^2 \ln \frac{r_S - R\cos\psi + l_{SR}}{R - R\cos\psi + l} \right.$$

$$\left. - \frac{R^2H}{l} \left[1 + \frac{H}{R} + \frac{1}{3} \left(\frac{H}{R} \right)^2 \right] \right\}$$
(10)

where γ is the normal gravity on the geoid and

$$r_S = R + H \tag{11a}$$

$$l_{SR} = \sqrt{r_S^2 - 2Rr_S\cos\psi + R^2}$$
 (11b)

$$l = l_{GP} = R\sqrt{2(1 - \cos\psi)}$$
 (11c)

The DTE is defined as the gravity difference between the topography and the condensed layer at the Earth's surface. It can be

function (ibid.)

$$k_{DTE} = \frac{r_{S}r_{P}(1 - 6\cos^{2}\psi) + (3r_{P}^{2} + r_{S}^{2})\cos\psi}{l_{SP}} + \frac{Rr_{P}(1 - 6\cos^{2}\psi) + (3r_{P}^{2} + R^{2})\cos\psi}{l_{RP}} - (-1 + 3\cos^{2}\psi)r_{P}\ln\frac{r_{S} - r_{P}\cos\psi + l_{SP}}{R - r_{P}\cos\psi + l_{RP}} - \frac{r_{P} - R\cos\psi}{l_{RP}^{2}}HR^{2}[1 + \frac{H}{R} + \frac{1}{3}(\frac{H}{R})^{2}]$$
(12a)

where

$$l_{RP} = \sqrt{r_P^2 - 2Rr_P\cos\psi + R^2}$$
 (12b)

3. Treatment of the singularities in the innermost column

For both the DTE and ITE, the singularities at the innermost column need to be treated. The size of the innermost column is small — for SRTM30, the base of the innermost column is a 30" \times 30" equal angular block (1 km \times 1 km at the Equator) and the planar approximation is adequate. Under the planar approximation, the innermost column becomes a rectangle prism with half base lengths of a and b along latitude and longitude directions, respectively. We assume the computation point to be located at center of the top or bottom of the prism for the direct and indirect effect, respectively. If the computation point P was chosen as the origin of a local coordinates system xyz (Nagy, et al., 2000), the potential of the innermost column is given by

$$\delta V_T = G\rho[xy\ln(z+l_0) + yz\ln(x+l_0) + zx\ln(y+l_0)]$$

$$-\frac{1}{2}\left(x^2 \tan^{-1} \frac{yz}{xl_0} + y^2 \tan^{-1} \frac{xz}{yl_0} + z^2 \tan^{-1} \frac{xy}{zl_0}\right) \Big]_{-a}^a \Big|_{-b}^b \Big|_{z_1}^{z_2}$$
(13)

where

$$l_0 = \sqrt{x^2 + y^2 + z^2}$$

$$z_1 = Z_P$$

$$z_2 = Z_P - H$$
(14)

 Z_P is the vertical distance between the computation point P and the geoid.

The vertical derivative of Eq. (13) is (ibid. Eq. (8))

$$\frac{\partial \delta V_T}{\partial z} = G \rho [x \ln(y + l_0) + y \ln(x + l_0) - z \tan^{-1} \frac{xy}{z l_0}]_{-a}^a \Big|_{-b}^b \Big|_{z_1}^{z_2}$$
(15)

The potential of the condensed surface layer is given by

$$\delta V_{S} = G\rho H \int_{-a}^{a} \int_{-b}^{b} \frac{1}{\sqrt{x^{2} + y^{2} + Z_{P}^{2}}} dx dy$$

$$= G\rho H \left[-Z_{P} \tan^{-1} \frac{xy}{Z_{P} \sqrt{x^{2} + y^{2} + Z_{P}^{2}}} + \right.$$

$$+ y \ln(x + \sqrt{x^{2} + y^{2} + Z_{P}^{2}})$$

$$+ x \ln(y + \sqrt{x^{2} + y^{2} + Z_{P}^{2}}) \left. \right|_{-a}^{a} \left. \right|_{-b}^{b}$$
(16)

Journal of Geodetic Science

and its vertical derivatives is

$$\frac{\partial \delta V_{S}}{\partial z_{P}} = G \rho H \left(\frac{x Z_{P}}{x^{2} + Z_{P}^{2}} + \frac{y Z_{P}}{y^{2} + Z_{P}^{2}} \right) \\
- \tan^{-1} \frac{x y}{Z_{P} \sqrt{x^{2} + y^{2} + Z_{P}^{2}}} \Big) \Big|_{-a}^{b} \Big|_{-b}^{b} \tag{17}$$

Based on the definition, the DTE and ITE of the innermost column are

$$\delta A_{DTE} = -\frac{\partial \delta V_T}{\partial z} + \frac{\partial \delta V_S}{\partial z}$$
 (18)

$$\delta N_{ITE} = \frac{\delta V_T - \delta V_S}{\nu} \tag{19}$$

Formulas for δV_T , δV_S and their derivatives can be formally written as general functions f(x, y, z) and $g(x, y, Z_P)$. They can be evaluated as:

$$f(x, y, z)|_{x_1}^{x_2}|_{y_1}^{y_2}|_{z_1}^{z_2}$$

$$= f(x_2, y_2, z_2) - f(x_2, y_2, z_1)$$

$$-f(x_2, y_1, z_2) + f(x_2, y_1, z_1)$$

$$-f(x_1, y_2, z_2) + f(x_1, y_2, z_1)$$

$$+f(x_1, y_1, z_2) - f(x_1, y_1, z_1)$$
(20)

and

$$g(x, y, Z_p)|_{x_1}^{x_2}|_{y_1}^{y_2}$$

$$= g(x_2, y_2, Z_p) - g(x_2, y_1, Z_p)$$

$$-g(x_1, y_2, Z_p) + g(x_1, y_1, Z_p)$$
(21)

As a demonstration, the contribution of the innermost column to the DTE and ITE is computed using the above equations at few selected points that have the highest, medium and lower elevations and are listed in the following table.

Table 1. Contributions of the innermost column to the DTE and ITE.

Latitude	Longitude	H (m)	DTE(mGal)	ITE (cm)
27.9792	86.9292	8685	51.9	-41.9
25.8792	270.2542	0	0.0	0.0
39.1958	270.2542	202	4.3	-0.2
39.1958	253.5208	4071	45.7	-16.7
-27.9875	290.3292	3077	46.3	-12.8

It is important to point out that the innermost column contributions are significant, even if its size is small. The computation point of the ITE is at the condensed layer that produces a slightly larger potential than the innermost column, and the difference between the two, namely the indirect topographic effect, is negative. For the DTE, the computation point is on the Earth's surface. The surface layer is at the bottom of the topography and produces slightly smaller attraction. Therefore, the DTE of the innermost column is positive.



Journal of Geodetic Science

4. Truncation errors

To speed up the computation, the global computations are limited to an area in which the specified computation accuracy is met. Thus the truncation error needs to be studied.

The truncation errors are usually discussed in the term of root mean squares or standard deviations. More stringently, we chose absolute maximum error as our criteria in this paper. We know the maximum topographic effect is in the highest mountain, so we compute the topographic effect at the highest point of the Himalaya mountain (H=8685m according to SRTM30) with different sizes of the computation areas. The DTE and ITE at this point are -235.9 cm and 196.2 mGal, respectively. The truncation errors due to different size of computation areas (equal angular blocks) are shown in the following tables.

Table 2. Truncation error of ITE Units in cm.

Block Size									
Trunc. Err.	111.2	12.8	8.9	7.3	5.7	4.0	1.6	0.7	0.3

Table 3. Truncation error of DTE Units in mGal.

Block Size	0.05°	0.5°	1°	2°	5°	10°	20°	30°	50°
Trunc. Err.	1.7	35.7	15.1	6.5	1.9	0.6	0.1	0.0	0.0

Table 2 shows that the contributions are mostly from the innermost zone. Almost half of the contributions come from an innermost block of 0.05° (less than a circle of 3 km in radius) for the indirect effect. When the size of the innermost block becomes of a half degree, the ITE is accounted for almost 95%. Unfortunately, the ITE decreases slowly after a very quick drop. If point-wise cm-accuracy is required, large computation area is required. In the above example, the computation area has to be extended into more than 30° to reach the 1-cm goal at the peak of the Himalayas.

The similar conclusions can be drawn for the direct effect. If the integration area is $10^{\circ} \times 10^{\circ}$, the truncation error is below 1 mGal. The truncation error falls below 0.1 mGal if a 20° computation area is used.

For 1D FFT computations, latitude bands are used. So we repeat above computations for latitude bands and the results are listed in Table 4 and 5.

The results are very similar to those computed in blocks. Table 4 shows that if the integration area is larger than or equal to 50° , the truncation error is below 0.1 cm. The truncation error of DTE is below 0.1 mGal if a 20° latitude band is used. To treat the direct and

VERSITA

Table 4. Truncation error of the ITE by latitude band (cm).

Band Size	0.05°	0.5°	1°	2°	5°	10°	20°	30°	50°
Trunc. Err.	70.2	9.8	7.5	6.3	4.7	2.9	0.7	0.3	0.1

Table 5. Truncation error of DTE by latitude band (mGal).

Band Size	0.05°	0.5°	1°	2°	5°	10°	20°	30°	50°
Trunc. Err.	31.9	18.2	7.4	3.3	1.1	0.3	0.0	0.0	0.0

ITE computations equally, the computations for both are limited to a 50° band.

5. Taylor expansions in the outer zone

As we showed in the previous section, a minim 50 degree of latitude band is needed to reach 0.1cm accuracy of ITE. When a DEM has very high resolution, such as the SRTM30, the numerical computations for such a large area are practically impossible — it requires years of computation time with today's computation power. In order to apply the most efficient FFT, the kernels of the integrals are expanded into Taylor series of a function of height. The series converges quickly in outer zones where height is much smaller than the distance. In the remainder of this section, we expand the kernel functions of the DTE and ITE into series of a function of height, using MATHEMATICA 4.

5.1. ITE in outer zone

Using Eqs. (10), (11a,b,c) and noting that

$$R - R\cos\psi = R(1 - \cos\psi) = \frac{\ell^2}{2R}$$
 (22)

$$l_{SR} = \sqrt{l^2 + \frac{l^2 H}{R} + H^2} = l\sqrt{1 + \frac{H}{R} + \frac{H^2}{l^2}},$$
 (23)

the ITE (10) is expanded into a series of \boldsymbol{H} as

$$k_{IND} = \left[\frac{3(1+\vartheta)l}{4} + \frac{c-R^2}{l}\right]H$$

$$+\left[-\frac{3(-1+\vartheta)l}{16R} + \frac{R(1+3\vartheta)}{4l} - \frac{c+4R^2}{4Rl}\right]H^2$$

$$+\left[\frac{(-1+3\vartheta)(l^2-4R^2)l^2}{32} + \frac{c(-4R^2+3l^2)-8l^2R^2}{24}\right]\frac{1}{R^2l^3}H^3$$

$$+\left[\frac{(-4R^2+l^2)[3(-1+5\vartheta)l^2-4(1+3\vartheta)R^2]}{256} + \frac{c(12R^2-5l^2)}{64}\right]\frac{1}{R^3l^3}H^4$$

$$+\left[\frac{(-4R^2+l^2)[3(-1+7\vartheta)l^2-4(1+9\vartheta)R^2]}{512} + \frac{c(48R^4+35l^4-120R^2l^2)}{640l^2}\right]\frac{1}{R^4l^3}H^5$$

$$+O(H^6)$$
(24)

where we have used

$$\vartheta = \cos \psi,$$
 $c = \frac{R^2}{2}(-1 + 3\vartheta^2)$ (25)

and $O(H^6)$ includes all terms containing H^6 and higher orders.

Notice that function ϑ can be written into a function of distance I using Eq. (22). Thus, each term in (24) becomes a convolution of functions of I and H and their higher powers, so 1D FFT can be applied.

To estimate the magnitude of the terms numerically, we compute the contribution of each term at selected points having the highest and some lower elevations.

Table 6. Contributions of different powers of height in the outer zone that is the globe minus the $0.5^{\circ} \times 0.5^{\circ}$ inner zone. Units in cm

Latitude	Longitude	Elev.	Н	H^2	H^3	H^4	H^5
27. 9792	86.9292	8685	0.0	-8.4	-5.8	0.0	0.0
25.8792	270.2542	0	0.0	-2.1	0.0	0.0	0.0
39.1958	270.2542	202	0.0	-2.2	0.0	0.0	0.0
39.1958	253.5208	4071	0.0	-3.4	-1.9	0.0	0.0
-27.9875	290.3292	3077	0.0	-3.9	-2.7	0.0	0.0
-28.2375	290.3292	2999	0.0	-3.9	-2.9	0.0	0.0

Interestingly, the contribution of the linear term containing H is trivial to the indirect effect. This may due to the fact that the most contribution comes from the inner zone and the linear terms of the topography and the condensed surface layer are very close. The H^3 term has meaningful contributions only in high mountains regions. Based on the results in Table 6, terms of H^2 and H^3 are computed only.

5.2. DTE in outer zone

After some simple algebraic operations on Eq. (12b), we have

$$\cos \psi = \frac{r_P^2 + R^2 - l_{RP}^2}{2Rr_P}$$
 (26a)

Substituting r_S in Eq. (3) by (11a), we obtain

$$l_{SP} = \sqrt{l_{RP}^2 + 2H(R - r_P \cos \psi) + H^2}$$

$$= l_{RP} \sqrt{1 + \frac{2H}{l_{RP}^2} (R - \frac{r_P^2 + R^2 - l_{RP}^2}{2R}) + \frac{H^2}{l_{RP}^2}}$$

$$= l_P \sqrt{1 + \frac{2H}{l_P^2} (R - \frac{r_P^2 + R^2 - l_P^2}{2R}) + \frac{H^2}{l_P^2}}$$
(26b)

where we have abbreviated l_{RP} by l_P .

Inserting Eqs. (26a), (26b) into (12a) and using the "Series" followed by the "Simplify" functions of MATHMATICA 4, we finally obtain:

$$k_{DTE} = \frac{R^{2}(r_{P}^{2} - R^{2} + l_{P}^{2})}{2r_{P}l_{P}^{3}}H$$

$$+ \frac{R[3l_{P}^{4} + 3(r_{P}^{2} - R^{2})^{2} + l_{P}^{2}(2r_{P}^{2} - 6R^{2})]}{8r_{P}l_{P}^{5}}H^{2}$$

$$+ \frac{3l_{P}^{6} + 15(r_{P}^{2} - R^{2})^{3} + l_{P}^{4}(r_{P}^{2} - 21R^{2}) + 3l_{P}^{2}(11R^{4} - 10R^{2}r_{P}^{2} - r_{P}^{4})}{48r_{P}l_{P}^{7}}H^{3}$$

$$- \frac{8R^{2}l_{P}^{6} + l_{P}^{6} - 35(r_{P}^{2} - R^{2})^{4} - 6l_{P}^{4}(r_{P}^{4} - 2R^{2}r_{P}^{2} + 9R^{4}) + 40l_{P}^{2}(2R^{6} - 3R^{4}r_{P}^{2} + r_{P}^{6})}{128Rr_{P}l_{P}^{6}}H^{4}$$

$$+ \frac{1}{1280R^{2}r_{P}l_{P}^{11}}[3l_{P}^{10} + 315(r_{P}^{2} - R^{2})^{5} - l_{P}^{8}(r_{P}^{2} - 9R^{2})$$

$$-35l_{P}^{2}(r_{P}^{2} - R^{2})^{3}(19r_{P}^{2} + 21R^{2}) + 6l_{P}^{6}(13R^{4} + 2R^{2}r_{P}^{2} - 7r_{P}^{4})$$

$$-30l_{P}^{4}(17R^{6} - 7R^{4}r_{P}^{2} + 3R^{2}r_{P}^{4} - 13r_{P}^{6})]H^{5}$$

$$-\frac{r_{P} - R\cos\psi}{l_{P}^{3}}HR^{2}[1 + \frac{H}{R} + \frac{1}{3}(\frac{H}{R})^{2}] + O(H^{6})$$
(27)

To estimate the magnitude of the terms numerically, we compute the contribution of each term at the selected points.

Table 7. Contribution of different powers of height in the outer zone to the direct effect. Units in mGals.

Latitude	Longitude	Elev.	Н	H^2	H^3	H^4	H^5
27. 9792	86.9292	8685	0.0	-29.8	-1.9	0.1	0.0
25.8792	270.2542	0	0.0	-0.0	0.0	0.0	0.0
39.1958	270.2542	202	0.0	-0.1	0.0	0.0	0.0
39.1958	253.5208	4071	0.0	-17.3	-0.4	0.1	0.0
-27.9875	290.3292	3077	0.0	-19.8	-0.3	0.1	0.0
-28.2375	290.3292	2999	0.0	-21.4	-0.4	0.1	0.0

Again, the linear term of H is trivial, and the dominant term is H^2 . Term H^3 contributes only 1.9 mGal at the Himalayas and sub-mGals at other sites. Contributions of all other terms are under 0.1 mGal point wise at those selected points.

Each term is Eq. (27) is not convolution because the distance l_P is a function of H. In order to apply 1D FFT, l_P is approximated by l in Eq. (27). Retaining only terms of H^2 and H^3 , and noting that

$$r_P - R\cos\psi = r_P - R + R(1 - \cos\psi) = r_P - R + \frac{l^2}{2R}$$
 (28)

Eq. (27) is approximated by

$$k_{DTE} \approx \left(\frac{3}{8r_{P}} - \frac{1}{2R}\right) \frac{RH^{2}}{l} + \frac{R(-3r_{P}^{2} - 3R^{2} + 4hRr_{P})}{4r_{P}} \frac{H^{2}}{l^{3}} + \frac{3R(r_{P}^{2} - R^{2})^{2}}{8r_{P}} \frac{H^{2}}{l^{5}} + \left(\frac{1}{16r_{P}} - \frac{1}{6R}\right) \frac{H^{3}}{l} + \left(\frac{r_{P}^{2} - 21R^{2}}{48r_{P}} - \frac{r_{P} - R}{3}\right) \frac{H^{3}}{l^{3}} + \frac{11R^{4} - 10R^{2}r_{P}^{2} - r_{P}^{4}}{l^{6}r_{P}} \frac{H^{3}}{l^{5}} + \frac{15(r_{P}^{2} - R^{2})^{3}}{16r_{P}} \frac{H^{3}}{l^{7}}$$
(29)

Each term in (29) is a convolution of functions of I and H and their higher powers, so that 1D FFT can be applied. To show the accuracy of Eq. (29), we repeat the same computation Table 7 and the results are given the following Table 8.

Table 8. DTE computed using Eq. (29) in the outer zone. Units in

Latitude	Longitude	Elev.	H^2	Abs. Err.	H^3	Abs. Err.
27.9792	86.9292	8685	-31.3	1.5	-2.2	0.3
25.8792	270.2542	0	-0.0	0.0	0.0	0.0
39.1958	270.2542	202	-0.1	0.0	0.0	0.0
39.1958	253.5208	4071	-17.6	0.3	-0.5	0.1
-27.9875	290.3292	3058	-19.9	0.1	-0.3	0.0
-28.2375	290.3292	2999	-21.5	0.1	-0.4	0.0

The results in Table 8 show that the approximation formula is accurate up to sub-mGal in most cases. At the Himalayas Mountains, the errors of approximation reach 1.5 and 0.3 mGal for the terms of H^2 and H^3 , respectively. Based the results in Table 8, Eq. (29) is adopted for the outer zone direct-effect computations.

6. Computation results

There are over 933 million 30"x30" cells of the SRTM30. Excluding ocean areas, the mean and standard deviation are 1125 and 1157 meters, respectively. The maximum peak of the Earth's surface modeled by SRTM30 is 8685 meters in the Himalayan Mountains. Excluding the polar regions (-70° $\leq \varphi \leq$ 70°), the mean and standard deviation decrease to 670 and 838 meters, respectively.

The horizontal and vertical accuracy of the SRTM30 data is 20 and 16 m with a 90% confidence interval (Becker et al., 2009). However, there are still some unrealistic sudden jumps in this DEM. There are cells that abruptly rise or fall below neighboring cells by 3000 meters. The total number of cells that have slopes greater than 45° is 6660. Even though they represent a very small fraction of the total number of cells, they cause large errors at the location and surrounding cells. The situation becomes worse at high latitude

where the cell size along the longitude direction becomes much smaller due to the convergence of the meridian. It is plausible to assume that the maximum DTE and ITE are close to those in the Himalayas Mountains, so the maximum absolute DTE and ITE are limited to 3 meter and 300 mGals, and the outliers are flagged by 32767.

Computations took space in 4 SUN workstations at NGS. The computation time is around 10 days for the inner zones for indirect or direct effects. The outer zone computations took about the same time with workloads spread at 4 workstations. The follows are the results of the computed DTE and ITE. Since larger values of the DTE and ITE in the Polar Regions are produced by heights with poor quality and problems of the convergence of the prime meridian, the statistics are limited between latitude $\pm 70^{\circ}$. The topography is defined overland only. However, based on Newton's gravitational law, it has an impact everywhere. Thus we have DTE and ITE over oceans, even if does not have any practical meaning. For this reason, we give the statistics over land areas only.

Table 9. Statistics of ITE for land areas (area weighted) Units in cm.

Number	208353324
Mean	-6.4
STD	15.6
Min.	-235.9
Max.	-1.2

The ITE is negative everywhere. The extreme value is -235.9 cm at latitude 27.9792° and 86.9375° with height 8685 m. It is worthwhile to point out that the global average of ITE is negative and non-zero. If the zero mean is enforced, the geocenter shift may occur (Martinec, 1998). Because Stokes function does not contain those harmonic degrees, so that the contribution of DTE to the geoid does not contain those harmonic degrees. If the geoid is computed under the Stoke-Helmert scheme, the zero and first degree of spherical harmonics are not compensated. Proper treatment of the mean values in the direct and ITE needs to be dealt carefully.

Grushinsky's formula is the first order approximation of the ITE (Wichiencharoen, 1982, p. 25). To illustrate the error of the linear approximation, we draw the ITE of Grushinsky's formula and the one computed in this paper along a parallel latitude band across the Himalayas in the figure 1.

Figure 1 clearly shows that the ITE computed in this paper is smoother than that of Grushinsky's. The blue curve is the difference between the computed and that computed by Grushinsky's formula, namely the error of the linear approximation. This error

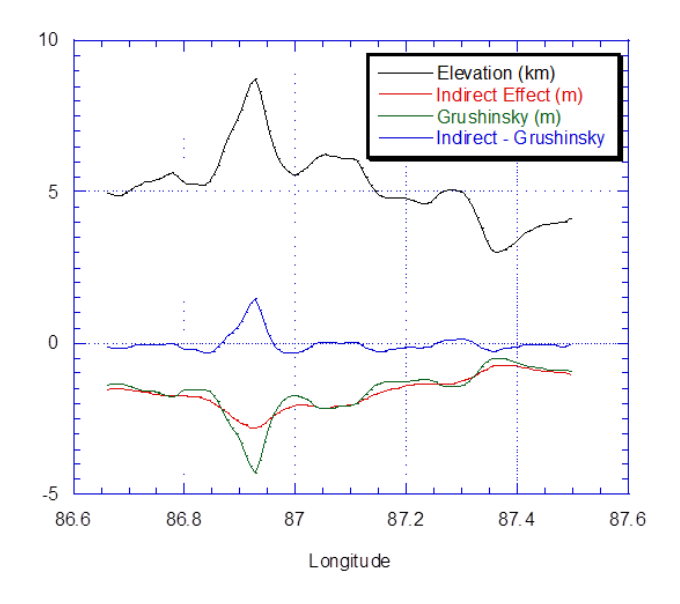


Figure 1. ITE along latitude 27.9792°.

exceeds 1.7 meter at the peak, then fluctuates around 30 cm in the region.

The statistics of the DTE are given in the following table.

Table 10. Statistics of the DTE for land areas (area weighted) Units in mGal.

Number	205991612
Mean	-0.8
STD	7.6
Min.	-274.3
Max.	195.3

Unlike the ITE which is negative everywhere, the DTE changes signs. The extreme value of -274.3 mGal happens at latitude -13.5625° and longitude 289.4875° with height of 1426 m, due to very rapid height rise of more than 800 meters in the neighboring cells (1 km grid spacing). This large value of DTE implies that not only the height, but also the slopes of height play a critical role in computing the direct effect. The maximum DTE is 195.3 mGal and is located at latitude 27.8958° and longitude 87.1125°, near the peak of the Himalayan Mountains.

For the Conterminous United States (CONUS), the mean and standard deviation of the ITE are -4.2 and 6.0 cm, respectively. The minimum value is -80.5 cm and is located at latitude 39.3333° and longitude 253.8833°. The maximum difference from the ITE of Grushinsky is 42.7 cm. The RMS value of overall difference is

1.4 cm. The mean and standard deviation of DTE over CONUS are -0.9 and 4.9 mGal, respectively. The extreme values are -135.9 mGal at latitude of 24.0° and longitude of 254.4167° . Again, large mean value of the ITE (-4.2 cm) over CONUS calls for attention, if cm-geoid accuracy is required.

7. Conclusions

The studies of DTE and ITE to the geoid computations are abundant in geodetic literatures (e.g., Martinec and Vanicek, 1994 a, b; Vanicek et al., 1999). In this paper, the DTE and ITE of Helmert's 2^{nd} method of condensation are computed globally by using the digital elevation model SRTM30. In order to make the computation possible and keep high computation accuracy (0.1 mgal and 0.1 cm for direct and indirect effect, respectively), we split the computation area into an inner zone $(0.5^{\circ} \times 0.5^{\circ})$ and outer zone (rest of the globe). The closed formulas are used in the inner zone for high computation accuracy, and then expanded into Taylor series for the use of 1D FFT in outer zone computations.

Notice that the mean value of ITE is -6.4 cm over land areas. If the ITE is added to a geoid computed under the Stokes-Helmert scheme, the geoid will be 6.4 cm lower. The bias should be compensated by the procedure of "removing direct effect" and "adding indirect effect" under the Stokes-Helmert scheme. However, the Stokes function does not contain the zero and first degree spherical harmonics, thus those harmonics in the ITE are not compensated at all. Even if the long wavelengths of gravity field have been



accurately determined by satellite gravity models, the very long wavelengths in the geoid computed under the Stokes-Helmert scheme may be affected. How to treat the biases in the DTE and ITE in precise geoid computation under the Stokes-Helmert scheme is needed.

The DTE and ITE are -235.9cm and 195.3 mGal at the highest point on Earth. The RMS values of the DTE and ITE on land areas are ± 15.6 cm and ± 7.6 mGal, respectively. It is worthwhile to point out that the ITE computed in this paper is smoother than that computed from Grushinsky's formula which has been used as an approximation of the ITE to the geoid. The maximum difference reaches 171.5 cm at the highest point on Earth. For the United States, the maximum difference is 43.7 cm in the Rocky Mountains. For this reason, Grushinsky's formula should not be used for precise geoid computation.

References

Becker JJ, DT Sandwell, WHF Smith, J Braud, B Binder, J Depner, D Fabre, J Factor, S Ingalls, S-H Kim, R Ladner, K Marks, S Nelson, A Pharaoh, R Trimmer, J Von Rosenberg, G Wallace, P Weatherall., Global Bathymetry and Elevation Data at 30 Arc Seconds Resolution: SRTM30_PLUS, Marine Geodesy, 32:4, 355-371, 2009.

Heck B., 2003, On Helmert's methods of condensation. J Geod. 77:155-170

Martinec Z., Vanicek P., 1994 a: Indirect effect of topography in the Stokes-Helmert technique for a spherical approximation of the geoid. Manuscr. geod. 19, pp. 213-219.

Martinec Z., Vanicek P., 1994b: Direct topographical effect of Helemert's condensation for a spherical approximation of the geoid. Manuscr. geod. 19, pp. 257-268.

Martinec Z., 1998, Boundary value problems for gravimetric determination of a precise geoid. Lecture notes in Earth Sciences, 73, Springer, Berlin Heidelberg New York.

Moritz H., 1968, On the use of the terrain correction in solving Molodensky's problem. Rep 108, Department of Geodetic Sci-

ence, The Ohio State University, Columbus.

Nagy D., G. Papp, and J. Benedek: 2000 The potential and its derivatives for the prism. J Geod, 74/7-8, 552 - 560.

Sjöberg L.E., Nahavandchi H., 1999, On the indirect effect in the Stokes—Helmert method of geoid determination. J Geod 73(2): 87-93.

Smith D.A., D. S. Robertson and D. G. Milbert, 2001, Gravitational attraction of local crustal masses in spherical coordinates, J Geod 74(11/12):783-789.

Vanicek P., Huang J., Novak P., Pagiatakis S., Veronneau M., Martinec Z., 1999,: Determination of the boundary values for the Stokes-Helmert problem. Journal of Geodesy, 73, pp. 180-192.

Wichiencharoen C., 1982, The indirect effects on the computation of geoid undulations. Report 336, Department of Geodetic Science, The Ohio State University, Columbus.

Appendix

The sign in the legalism function of Eq. (2) is unnecessary, since the following holds:

$$r_S - r_P \cos \psi + l_{SP} \ge 0$$
 (A1)

Inequality (A1) is easy to prove. Assume the opposite is true, that is:

$$r_S - r_P \cos \psi + l_{SP} < 0$$
, (A2)

then the following must be true:

$$r_P \cos \psi - r_S > l_{SP} \ge 0$$
 (A3)

Noting that

$$l_{SP}^2 = r_S^2 - 2r_S r_P \cos \psi + r_P^2$$
, (A4)

and using the square of (A3), we obtain

$$r_P^2 < r_P^2 \cos^2 \psi$$
 (A5)

Since $\cos^2\psi\leq 1$, inequality (A5) cannot be true, thus proving (A1). In the same way it can be proven that $r_G-r_P\cos\psi+l_{GP}\geq 0$. Thus the absolute sign in the legalism function is not needed.

